DMD Fast Forward. Published on March 30, 2011 as doi:10.1124/dmd.111.038224

The Application of Physiologically Based Pharmacokinetic Modelling to Understanding the Clinical Pharmacokinetics of UK-369,003.

Kenny J Watson, John Davis and Hannah M Jones.

Department of Pharmacokinetics, Dynamics and Metabolism, Pfizer Worldwide R&D (KJW, HMJ), Ramsgate Road, Sandwich, Kent, CT13 9NJ, UK.
Department of Clinical Pharmacology, Pfizer Worldwide R&D (JD), Ramsgate Road, Sandwich, Kent, CT13 9NJ, UK.

DMD Fast Forward. Published on March 30, 2011 as DOI: 10.1124/dmd.111.038224
This article has not been copyedited and formatted. The final version may differ from this version.

Running title

Application of PBPK modelling to UK-369,003 clinical PK.

Corresponding Author

Hannah M Jones

Department of Pharmacokinetics, Dynamics and Metabolism,

Pfizer Worldwide R&D,

Ramsgate Road,

Sandwich,

Kent.

CT13 9NJ,

UK.

E-mail : Hannah.jones@pfizer.com

Telephone : 01304 644207

Number of text page = 15

Number of tables = 3

Number of figures = 14

Number of references = 17

Number of words in abstract = 244

Number of words in introduction = 542

Number of words in discussion = 1499

Abbreviations used

ACAT = Advanced Compartmental Absorption and Transit; CAT = Compartmental Absorption and Transit; CL = clearance; CL_R = renal clearance; C_{ent} = enterocyte concentration; CYP3A4 = cytochrome P450 3A4; FaSSIF = Fasted State Simulated Intestinal Fluid; IV = intravenous;

DMD Fast Forward. Published on March 30, 2011 as DOI: 10.1124/dmd.111.038224
This article has not been copyedited and formatted. The final version may differ from this version.

PDE_5 = phosphodiesterase type 5; P-gp = P-glycoprotein; V_{dss} = steady state volume of distribution.

DMD Fast Forward. Published on March 30, 2011 as DOI: 10.1124/dmd.111.038224
This article has not been copyedited and formatted. The final version may differ from this version.

Abstract

UK-369,003 is a phosphodiesterase-5 inhibitor in clinical development at Pfizer. UK-369,003 is predominantly metabolised by cytochrome P450 3A4 and is also a substrate for the efflux transporter P-glycoprotein. The pharmacokinetics of UK-369,003 have been profiled following oral administration of 1 to 800mg of an immediate release formulation to healthy volunteers. Non-linearity was observed in the systemic exposure at doses of 100mg and greater. In addition, the pharmacokinetics of UK-369,003 have also been investigated following oral administration of the more therapeutically attractive modified release formulation. The modified release formulation prolonged systemic exposure, but offered a reduced bioavailability in comparison with the immediate release formulation. Physiologically based pharmacokinetic modelling strategies are commonly used in drug discovery and development. This work describes the application of the PBPK software GastroPlus™ in understanding the pharmacokinetics of UK-369,003. The impact of gut wall and hepatically mediated CYP3A4 metabolism, in addition to the actions of P-glycoprotein, in causing the non-linear pharmacokinetics of the immediate release formulation, and the reduced bioavailability of the modified release form, was investigated. The model accurately described the systemic exposure of UK-369,003 following intravenous and both immediate and modified release oral administration and suggests that CYP3A4 is responsible for the majority of the non-linearity in systemic exposure observed following administration of the immediate release form. Conversely, the reduced bioavailability of the modified release formulation is believed to be caused by incomplete release from the device, incomplete absorption of released drug and, to a lesser extent, CYP3A4 metabolism.

DMD Fast Forward. Published on March 30, 2011 as DOI: 10.1124/dmd.111.038224
This article has not been copyedited and formatted. The final version may differ from this version.

Introduction

UK-369,003 is a phosphodiesterase-5 (PDE_5) enzyme inhibitor in clinical development at Pfizer. UK-369,003 is a moderately lipophilic (Log $D_{7.4}$ = 2.4), weakly basic (pKa = 6.6) compound, the structure of which is presented in Figure 1.

UK-369,003 is moderately soluble and demonstrates high flux across Caco-2 cell monolayers. Consistent with these properties, UK-369,003 exhibits high absorption in pre-clinical pharmacokinetic studies. In vitro incubations performed in baculovirus cells engineered to individually express a range of CYP450 enzymes showed CYP3A4 to be responsible for the majority of the metabolism of UK-369,003. Three major metabolic pathways were identified; namely N-deethylation and N,N-deethylation of the N-ethylpiperazine in addition to O-demethylation of methoxyethyl sidechain. Ketoconazole (a CYP3A4 inhibitor) gave a significant, concentration dependant reduction in the rates of formation of each of these metabolites in vitro, further substantiating the role of CYP3A4 in the metabolism of UK-369,003. In addition to those experiments performed to understand its metabolic profile, studies performed in MDR-1 transfected MDCK cell lines indicate that UK-369,003 is a substrate for the efflux transporter P-glycoprotein (P-gp) (Km = 24μM).

The clinical pharmacokinetics of UK-369,003 have been profiled following intravenous (IV) and oral (PO) administration to healthy volunteers. All clinical studies discussed here were performed in the fasted state. Plasma concentration-time profiles observed following IV, immediate release (IR) and modified release (MR) oral administration are summarised in Figure 2. Following IV administration UK-369,003 demonstrated a moderate clearance (CL = 60L/hr) and steady state volume of distribution (V_{dss} = 2.4L/kg). UK-369,003 was found to have a renal clearance of 4.9L/hr. Following administration 100mg of UK-369,003 in an IR formulation a bioavailability 34% was observed. Considering the clearance of UK-369,003 (60L/hr) in comparison with hepatic blood flow (approximately 87L/hr; (Davies and Morris, 1993)), this is consistent with complete absorption from the gastrointestinal tract. A supra-proportional increase in systemic exposure was observed at doses greater than 100mg of the

DMD Fast Forward. Published on March 30, 2011 as DOI: 10.1124/dmd.111.038224
This article has not been copyedited and formatted. The final version may differ from this version.

IR formulation (Figure 2D).The PK of UK-369,003 has also been investigated following oral administration of a therapeutically more attractive MR formulation. As anticipated, the MR formulation prolongs the exposure and extends the terminal half-life of UK-369,003 (Figure 2E). In comparison with the IR form, a reduced bioavailability of the MR form is observed (18 vs 34%) following administration of 50, 100 and 200mg doses.

The use of physiologically based pharmacokinetic (PBPK) modelling strategies in drug discovery and development is becoming increasingly more commonplace (Parrott and Lave, 2002; Jones et al., 2006; De Buck et al., 2007; Germani et al., 2007; Jones et al., 2009; Parrott et al., 2009; Zhang et al., 2011; Rowland et al., 2011). This work describes the PBPK modelling undertaken to examine the pharmacokinetics of UK-369,003. The role of both gut wall and hepatically mediated CYP3A4 metabolism, along with gut mediated P-gp efflux, will be investigated using the physiologically based GastroPlus™ simulation software. This work aims to investigate the causes of the non-linearity in oral exposure observed following IR administration, in addition to investigating the cause of the reduced bioavailability of the MR formulation. Improved understanding of the kinetics of UK-369,003 will allow for more informed decisions making a in the clinical development of this candidate. For example, the model may be used to ensure appropriate delivery via the MR device in addition to educating the drug-drug interaction (DDI) studies required to underwrite progression of this candidate.

DMD Fast Forward. Published on March 30, 2011 as DOI: 10.1124/dmd.111.038224
This article has not been copyedited and formatted. The final version may differ from this version.

Methods

Physiologically Based PK Model.

GastroPlus™ (SimulationsPlus, Inc. CA) is a commercially available software which is routinely used to model drug absorption. The model underlying the prediction of absorption in GastroPlus™ is known as the Advanced Compartmental Absorption and Transit (ACAT) model (Agoram et al., 2001). The physiologically based ACAT model consists of nine compartments corresponding to different segments of the digestive tract and is based on the original CAT model described by Yu and Amidon (Yu et al., 1996). Each compartment is further subdivided to describe drug which is unreleased (when simulating modified release formulations), in addition to that which is undissolved, dissolved and absorbed. Absorbed drug is defined as drug which has entered into the enterocyte. Movement of drug between each sub-compartment is described by a series of differential equations. The rate of drug flow through sequential intestinal compartments is determined by the transit time of each compartment. All simulations were performed in GastroPlus™ v6.0. Input parameters used for this modelling are summarised in Table 1.

Only drug in solution is available for absorption. The solubility profile of UK-369,003 throughout the gastrointestinal tract was simulated by incorporation of the in vitro solubility in a biorelevant Fasted State Simulated Intestinal Fluid (FaSSIF) media, in combination with the ionisation state of the basic moiety as modulated by the regional pH in the gastrointestinal tract. The effective passive permeability of UK-369,003 was predicted from flux in Caco-2 cells in the presence of P-gp inhibitors. Passive absorption is assumed to be driven by the concentration gradient of the drug across the luminal membrane in an unsaturable manner. The model utilises an understanding of the abundance of both intestinal and hepatic CYP3A4 and gut P-gp to allow simulation of non-linear metabolism and P-gp efflux. It is assumed that carrier mediated active transport is described by Michaelis-Menten kinetics and is therefore saturable. Similarly, CYP3A4 metabolism was modelled according to Michaelis-Menten kinetics. A well-stirred venous equilibrium model where the unbound exposure in the liver is

assumed to be equivalent to the unbound systemic exposure at steady state was used to describe hepatocyte drug concentrations, while gut mediated metabolism and active transport were driven by predicted enterocyte concentrations.

Disposition following intravenous administration.

The PK of UK-369,003 has been investigated following IV administration of 10, 30 and 50mg to 5, 17 and 5 male healthy volunteers respectively. The disposition of UK-369,003 at these doses was modelled using a 2-compartmental fit in the GastroPlus™ PKPlus module. Simultaneous fitting of all dose groups was performed, assuming linearity in PK across the dose range profiled. A Hooke & Jeeves pattern search optimisation with proportional residual error structure was employed.

Pharmacokinetics following IR oral administration.

The PK of UK-369,003 has been investigated following administration of 1, 3, 10, 30, 100, 200, 400 and 800mg to 8 healthy male volunteers respectively. Using the GastroPlus optimisation tool the contribution of gut and hepatic CYP3A4 metabolism, and the impact of P-gp efflux on the PK of UK-369,003 was investigated. IV and IR PO profiles were modelled simultaneously, ensuring compatibility of the model with each route of administration. The ACAT model uses the input parameters listed in Table 1 to estimate the solubility, dissolution and passive absorption of UK-369,033 in each region of the gastrointestinal tract. These parameters are fixed in the model. A Hooke & Jeeves pattern search optimisation and proportional residual error structure was again employed. Three alternative models were investigated, namely the ‘CYP3A4’, ‘P-gp’ and ‘Combined’ models.

The ‘CYP3A4’ model assumes that non-linearity in IR plasma kinetics is mediated only by non-linear CYP3A4 metabolism. The impact of gut and liver metabolism was investigated by

estimation of CYP3A4 enzyme kinetics (V_{max} & K_m). In this model the distribution of UK-369,003 was assumed to be the same as estimated following IV administration.

The 'P-gp' model assumes that all non-linearity in IR plasma kinetics is mediated by P-gp only. The impact of non-linear gut mediated P-gp efflux was investigated by estimation of efflux kinetics (V_{max} & K_m). In this model, it was assumed that metabolic extraction of UK-369,003 remains unsaturated over the dose range investigated. As a result, both the clearance and distribution of UK-369,003 were assumed to be equivalent to that estimated following IV administration.

Finally, the 'Combined' model assumes that the non-linearity in IR plasma kinetics is due to a combination of both non-linear CYP3A4 metabolism and P-gp efflux. The impact of gut and liver mediated CYP 3A4 metabolism, in addition to gut mediated P-gp efflux, was investigated by estimation of both metabolic and efflux kinetics (V_{max} & K_m). As with the 'CYP3A4' model, the distribution of UK-369,003 was assumed to be the same as that estimated following IV administration.

Pharmacokinetics following modified release oral administration.

The PK of the MR formulation of UK-369,003 has been profiled following oral administration of 50, 100 and 200mg to respectively. Subsequent interrogation of the MR profiles was undertaken assuming that the ADME profile of UK-369,003 upon release from the MR device was as described by the 'Combined' model.

Previous clinical experience with the MR device used in these studies indicates that its passage through the gut may be considerably slower (mean = 34h; unpublished data) than the fasted gut transit time implemented within the standard ACAT model (21h). As a result, the default ACAT model was altered to ensure that the total gut transit time was reflective of the observed transit time. The relative transit through each compartment (excluding the stomach) was conserved i.e. the transit time of each compartment was increased

proportionally. The release of UK-369,003 from the device was described by the Weibull function shown in Equation 1.

$$\%\ released = 100 * \left(1 - \exp^{\left[-(Time-Lag)^{(Shape/Scale)}\right]}\right) \quad \text{(Equation 1)}$$

Lag, Shape and Scale parameters were estimated in parallel using the MR clinical data in the model. A Hooke & Jeeves pattern search optimisation with proportional residual error structure was again employed.

Model assumptions.

Implicit within each of these models are the following assumptions,

- The distribution and clearance kinetics of UK-369,003 are equivalent following both PO & IV administration.
- Where appropriate ('CYP3A4' model and 'Combined' model), the metabolism of UK-369,003 is assumed to be occurring only in the liver and gut wall, and is mediated solely by CYP3A4. Differences in gut and liver V_{max} are accounted for by tissue weight and CYP3A4 abundance only. CYP3A4 unbound $K_{m\ liver}$ = unbound $K_{m\ gut}$.
- When assuming P-gp to be the sole cause of the non-linearity ('P-gp model') elimination occurs only in the liver and is linear across the dose range investigated.
- The abundance and distribution of CYP3A4 contained within GastroPlus is physiologically relevant (Paine et al., 1997).
- Where appropriate ('P-gp' model and 'Combined' model) the role of P-gp is limited to the gut wall, and operates solely as an efflux transporter.
- The relative activity of P-gp through the gastrointestinal tract which is implemented in GastroPlus is physiologically accurate (Makhey et al., 1998).
- The in vitro solubility profile is predictive of the in vivo situation.

- Human passive permeability can be accurately predicted from in vitro Caco-2 data, in the presence of P-gp inhibitors.
- With the exception of the actions of P-gp in the gut wall, the absorption and distribution of UK-369,003 is assumed to be passive.
- UK-369,003 is subject to a renal clearance (Cl_r) of 4.9L/kg.

DMD Fast Forward. Published on March 30, 2011 as DOI: 10.1124/dmd.111.038224
This article has not been copyedited and formatted. The final version may differ from this version.

Results

Intravenous pharmacokinetics.

Figure 3 shows the predicted PK profiles of UK-369,003 estimated by simultaneous fitting of 10, 30 & 50mg doses. Each is superimposed on the observed clinical data ($^{+}/_{-}$ standard deviation). Corresponding goodness of fit plots are presented in Figure 4. When considering both Figures 3 and 4 it is clear that the disposition of UK-369,003 has been well described by a 2-compartment kinetic model. As a result of the relatively narrow dose range investigated, adequate description of the data is achieved assuming linear kinetics across all doses. Table 2 summarises the PK parameters estimated from this model, confirming the moderate clearance and distribution of UK-369,003.

Immediate release oral pharmacokinetics.

Figures 5, 6, and 7 show the predicted PK profiles of UK-369,003 estimated by simultaneous interrogation of IV and IR oral kinetics by 'CYP3A4', 'P-pg' and 'Combined' models respectively. Each is superimposed on the observed mean clinical data ($^{+}/_{-}$ standard deviation). Corresponding goodness of fit plots are presented in Figure 8.

When considered together, Figures 5 and 8A & B demonstrate that the non-linearity in systemic exposure observed following administration of IR UK-369,003 can be well described by assuming CYP3A4 is the sole perpetrator of the observed non-linearity. In contrast, Figures 6 and 8D highlights that P-gp is unlikely to be the sole cause of the non-linearity. This is exemplified by an over-estimation of systemic exposure observed at low dose (1mg; Figure 6A) and under-estimated exposure noted with the 800mg dose (Figure 6H). The increased precedence of under-estimating systemic exposure using the 'P-gp' model is highlighted by comparison of the goodness of fit plots presented in Figures 8A and 8B. Visual inspection of the model predicted exposure profiles achieved using the 'Combined' model (Figure 7)

suggests little improvement over the 'CYP3A4' model (Figure 5). Similarly, the goodness of fit plots presented in Figures 8A and 8E suggest little difference between either model. Table 3 presents a summary of the kinetic parameters, in addition to the objective goodness of fit measures (R^2, Aikake and Objective Function), returned by each of the models. Comparison of the objective measures associated with 'CYP3A4' and 'P-pg' models reconfirms the significant improvement in the model fit offered by the 'CYP3A4' model (increased R^2 and decreased Aikake and Objective Function) despite an equal number of estimated parameters. Subsequent comparison of 'CYP3A4' and 'Combined' models again suggests that there is no significant difference in the description of the observed data by either model. For example, the R^2 returned by each is identical, while the addition of 2 further parameters in the 'Combined' model (ie. P-gp V_{max} and K_m) results in a drop in objective function of only 0.72 – indicating redundancy of the additional parameters in the 'Combined' model.

Modified release oral pharmacokinetics.

Figure 9 presents MR profiles generated by incorporating the predicted release profile and increased gut transit time into the 'Combined' model. Although the 'CYP3A4' model provides an adequate description of the IR kinetics, the MR kinetics were interrogated using the 'Combined' model – see discussion for full explanation. The observed clinical data ($^{+}/_{-}$ standard deviation) is presented for comparison. Corresponding goodness of fit plots are presented in Figure 10, confirming the accurate description of the observed systemic exposures. In addition, the predicted release profile from the MR device is presented in Figure 11.

DMD Fast Forward. Published on March 30, 2011 as DOI: 10.1124/dmd.111.038224
This article has not been copyedited and formatted. The final version may differ from this version.

Discussion

Modelling and simulation approaches are increasingly being employed to guide the clinical development of drug candidates. Precedence for using such techniques, particularly GastroPlus, to justify clinical trial design has already been established. For example, simulations performed with multiple weak acidic and basic BCS Class II compounds have successfully justified biowavers for those candidates, negating the regulatory requirement to perform these studies (Tubic-Grozdanis et al., 2008). In addition, similar simulations for Etoricoxib have been used to support an assertion of equivalence between different IR solid oral formulations (Okumu et al., 2009).

The clinical PK of UK-369,003 has been described following both IV and oral administration of IR and MR formulations using a PBPK model. In vitro studies suggest that UK-369,003 is metabolised by CYP3A4 and is also a substrate for the P-gp efflux transporter. Therefore, this work was performed to investigate whether the non-linearity in plasma exposure observed following oral administration of the IR formulation was most likely due to saturation of gut and/or hepatically mediated CYP3A4, or gut mediated P-gp efflux. Furthermore, the cause of the reduced bioavailability observed with the MR form, in comparison with the IR form, has been investigated. In a similar manner, GastroPlus has previously been used to deconvolute the active transport mediated non-linearity in the PK of UK-343,664, Valacyclovir, Gabapentin and Talinolol (Abuasal et al., 2010; Tubic et al., 2006; Bolger et al., 2009). Modulation of the PK and pharmacodynamic endpoints of Adinazolam and Metoprolol by MR devices has also been successfully described (Lukacova et al., 2009).

As discussed, comparison of Figures 5-8 and the objective function measures (Table 3) indicates that the majority of the non-linearity observed following administration of the IR formulation can be attributed to the saturation of CYP3A4 metabolism. In addition to understanding the relative importance of CYP3A4 and P-gp in causing the non-linearity in plasma exposure, it is possible to examine the model further to determine the absolute contributions of both gut and hepatic CYP3A4 to the metabolism of UK-369,003. Figure 12

summarises the fraction of each dose which remains unabsorbed, or is removed by either gut wall or hepatic extraction. Essentially, UK-369,003 is completely absorbed at all doses, except following administration of 800mg where 10% of the dose remains unabsorbed. The high fraction absorbed is consistent with the high permeability and solubility of UK-369,003 (Table 1) and complete absorption observed in preclinical PK studies. The simulations suggest that the relative contributions of gut and liver metabolism to the extraction of UK-369,003 change with dose (Figure 12). At the lowest doses investigated the gut wall plays a major role in the exclusion of UK-369,003 from the systemic circulation; approximately 50% of a 1mg dose is removed by the gut wall. However, gut wall extraction is rapidly saturated upon increasing dose; only 10% of administered 30mg dose is extracted by the gut.

The largest proportion of the dose (~60%) is predicted to be absorbed from the jejunum following administration of the IR formulation. Figure 13 contrasts the enterocyte concentrations (C_{ent}) simulated in the jejunum with the model predicted CYP3A4 K_m. The rapid saturation which is predicted in gut wall metabolism results from the predicted enterocyte exposure profiles of UK-369,003 being significantly in excess of the K_m in all but the lowest dose investigated. Conversely, saturation of hepatic metabolism occurs to a lesser extent with increasing dose; a significant reduction in the fraction of the dose removed by the liver occurs only at higher doses (Figure 12). This is again reflected by comparing the free hepatic concentrations and predicted K_m (Figure 13) which demonstrate that simulated free exposure in the liver only reaches equivalence with the predicted K_m at doses of 100mg and greater. Overall, the model suggests that a rapid saturation of gastrointestinal metabolism occurs with increasing dose (1 – 30mg), during which time the fraction removed by hepatic metabolism increases to compensate. As such, no significant non-linearity in plasma kinetics is observed until the saturation of hepatic extraction becomes prevalent (dose ≥ 100mg).

The bioavailability of the MR form (18%) is reduced in comparison with the IR form. Previous clinical experience demonstrates that the mean transit time of the MR device used in these studies is approximately 34h. Visual inspection of the concentration-time profiles observed following administration of the MR form (Figure 2) indicates that the extended half-life of the

MR form is maintained at times in excess of the standard gut transit time of the ACAT model (21h); further substantiating the hypothesis that absorption is continuing in excess of this time. Therefore, the ACAT model was modified when interrogating the MR PK profiles in order to maintain its physiological relevance.

Whilst recognising that the 'CYP3A4' model offers an adequate description of the IR oral pharmacokinetics, the MR profiles were modelled using the 'Combined' model. The decision to employ the 'Combined' model was taken to reflect the different absorption profiles of both formulations. As UK-369,003 is a highly permeable candidate, the absolute mass of drug remaining to be absorbed in the lower intestine is comparatively low when considered in comparison with the MR form, where delayed release from the device increases the drug present in the colon (Figure 14). As the activity of P-gp incorporated into the GastroPlus PBPK model increases in the lower intestine (Makhey et al., 1998) the impact of P-gp on the absorption of the MR form may be greater than on the IR form. Furthermore, as the 'Combined' model derived estimate of P-gp K_m (39μM) is broadly similar to that measured in vitro (24μM), the likelihood of significant model misspecification caused by the inclusion of P-gp in the interrogation of MR forms is assumed to be minimal.

By integrating the optimised release profile of the MR device, along with the modified transit time into the 'Combined' model, the model accurately describes the PK of the MR formulation (Figure 11). The range of MR doses investigated clinically (50 – 200 mg) is much narrower than the IR dose range profiled and, as a result, no non-linearity in plasma exposure is observed. Interrogation of the simulations performed allows an understanding of the multi-factorial nature of the reduced bioavailability of the MR form. In contrast to the complete absorption of the IR formulation it is predicted that 40% of UK-369,003 remains unabsorbed at the doses investigated. When considered along with the predicted release profile of the MR device presented in Figure 11 (~75% released from the device by 34h) it appears that the unabsorbed UK-369,003 is composed of approximately equivalent fractions of unreleased and unabsorbed drug. The incomplete absorption of released drug which is predicted is due to differences in regional permeability consistent with the physiology of the gastrointestinal

tract, P-gp efflux in the lower intestine (as a result of delayed absorption, resulting in increased exposure to P-gp in the lower intestine) and the physiochemical properties of UK-369,003 (Agoram et al., 2001; Ungell et al., 1998).The simulations suggest that gut wall metabolism has limited impact on the systemic exposure of the MR form (5% extraction at the doses investigated). While seemingly counterintuitive (given the lower enterocyte concentrations arising from administration of MR in comparison with IR forms), this is likely driven by the regional distribution of CYP3A4 implemented in GastroPlus (Paine et al., 1997) where the abundance of CYP3A4 is lowest in the lower intestine and colon. As a result of the sustained release from the MR device, the absolute mass of drug being exposed to drug metabolising enzyme in the upper intestine is reduced, and the contribution of metabolism to first pass is lowered accordingly. In summary, the simulations presented suggest the decreased bioavailability of the MR form to be multifactorial in nature; namely incomplete release from the MR device, incomplete absorption, P-gp mediated efflux and metabolic extraction (first pass metabolism) across both the gut wall and liver.

The capacity of the proposed model to quantitatively reflect the PK of IV, IR and MR forms greatly increases confidence in the physiological relevance of the simulations performed. To this end, the improved understanding of the kinetics afforded by the model allows it to be a useful tool for guiding clinical study design. For example, amalgamation of the DDI studies performed using the IR formulation along with increased understanding of the absorption and disposition of UK-369,003 afforded by this model, could enable timely estimation of the likely magnitude of DDIs which will be observed using the therapeutically preferred MR formulation.

In conclusion, the work presented here demonstrates the increased insight into the clinical kinetics of UK-369,003 which was gained by employing a PBPK model. These simulations suggest that the majority of the non-linearity in systemic exposure observed following administration of UK-369,003 in an IR form is mediated by saturation of both gut wall and hepatic CYP3A4, while the impact of P-gp is limited. The relative contribution of gut wall and hepatically mediated metabolism varies depending on the dose administered with the contribution of gut wall metabolism reducing rapidly with increasing dose. Furthermore,

DMD Fast Forward. Published on March 30, 2011 as DOI: 10.1124/dmd.111.038224
This article has not been copyedited and formatted. The final version may differ from this version.

reduced bioavailability of MR UK-369,003 is likely caused by incomplete release from the device and reduced absorption from the colon, in addition to a first pass extraction mediated by hepatic, and to a lesser extent, gut wall metabolism.

DMD Fast Forward. Published on March 30, 2011 as DOI: 10.1124/dmd.111.038224
This article has not been copyedited and formatted. The final version may differ from this version.

Acknowledgements.

The authors would like to thank Kevin Beaumont, Susan Cole, Anne Heatherington, Adriaan Cleton and Maurice Dickins for valuable scientific discussion of this work.

DMD Fast Forward. Published on March 30, 2011 as DOI: 10.1124/dmd.111.038224
This article has not been copyedited and formatted. The final version may differ from this version.

Authorship Contribution.

Participated in research design:	KJW, HMJ, JD
Conducted experiments:	
Contributed new reagents or analytical tools:	
Performed data analysis:	KJW, JD
Wrote or contributed to the writing of the manuscript:	KJW, HMJ

DMD Fast Forward. Published on March 30, 2011 as DOI: 10.1124/dmd.111.038224
This article has not been copyedited and formatted. The final version may differ from this version.

References.

Abuasal B, Walker D, Bolger M and Kaddoumi A (2010) In silico modelling for the non-linear absorption of P-Gp and CYP3A4 substrate UK-343,664. R6379. AAPS New Orleans.

Agoram B, Woltosz WS and Bolger MB (2001) Predicting the impact of physiological and biochemical processes on oral drug bioavailability. *Adv Drug Deliv Rev* **50** Suppl 1:S41-67.

Bolger MB, Lukacova V and Woltosz WS (2009) Simulations of the nonlinear dose dependence for substrates of influx and efflux transporters in the human intestine. *AAPS J* **11**:353-363.

Davies B and Morris T (1993) Physiological parameters in laboratory animals and humans. *Pharm Res* **10**:1093-1095.

De Buck SS, Sinha VK, Fenu LA, Nijsen MJ, Mackie CE and Gilissen RA (2007) Prediction of human pharmacokinetics using physiologically based modeling: a retrospective analysis of 26 clinically tested drugs. *Drug Metab Dispos* **35**:1766-1780.

Germani M, Crivori P, Rocchetti M, Burton PS, Wilson AG, Smith ME and Poggesi I (2007) Evaluation of a basic physiologically based pharmacokinetic model for simulating the first-time-in-animal study. *Eur J Pharm Sci* **31**:190-201.

Jones HM, Gardner IB and Watson KJ (2009) Modelling and PBPK simulation in drug discovery. *AAPS J* **11**:155-166.

Jones HM, Parrott N, Jorga K and Lave T (2006) A novel strategy for physiologically based predictions of human pharmacokinetics. *Clin Pharmacokinet* **45**:511-542.

Lukacova V, Woltosz WS and Bolger MB (2009) Prediction of modified release pharmacokinetics and pharmacodynamics from in vitro, immediate release, and intravenous data. *AAPS J* **11**:323-334.

Makhey VD, Guo A, Norris DA, Hu P, Yan J and Sinko PJ (1998) Characterization of the regional intestinal kinetics of drug efflux in rat and human intestine and in Caco-2 cells. *Pharm Res* **15**:1160-1167.

Okumu A, DiMaso M and Lobenberg R (2009) Computer simulations using GastroPlus to justify a bi owaiver for etoricoxib solid oral drug products. *Eur J Pharm Biopharm* **72**:91-98.

Paine MF, Khalighi M, Fisher JM, Shen DD, Kunze KL, Marsh CL, Perkins JD and Thummel KE (1997) Characterization of interintestinal and intraintestinal variations in human CYP3A-dependent metabolism. *J Pharmacol Exp Ther* **283**:1552-1562.

Parrott N and Lave T (2002) Prediction of intestinal absorption: comparative assessment of GASTROPLUS and IDEA. *Eur J Pharm Sci* **17**:51-61.

Parrott N, Lukacova V, Fraczkiewicz G and Bolger MB (2009) Predicting pharmacokinetics of drugs using physiologically based modeling--application to food effects. *AAPS J* **11**:45-53.

Rowland M, Peck C, Tucker G (2011) Physiologically-based pharmacokinetics in drug development and regulatory science. Annu Rev Pharmacol Toxicol 51: 45-73.

Tubic-Grozdanis M, Bolger MB and Langguth P (2008) Application of gastrointestinal simulation for extensions for biowaivers of highly permeable compounds. *AAPS J* **10**:213-226.

Tubic M, Wagner D, Spahn-Langguth H, Bolger MB and Langguth P (2006) In silico modeling of non-linear drug absorption for the P-gp substrate talinolol and of consequences for the resulting pharmacodynamic effect. *Pharm Res* **23**:1712-1720.

Ungell AL, Nylander S, Bergstrand S, Sjoberg A, Lennernas H (1998) Membrane transport of drugs in different regions of the gastrointestinal tract of the rat. *J Pharm Sci* **87**:1197-1240.

Yu LX, Lipka E, Crison JR and A midon GL (1996) Transport approaches to the biopharmaceutical design of oral drug delivery systems: prediction of intestinal absorption. *Adv Drug Deliv Rev* **19**:359-376.

Zhao P, Zhang L, Grillo JA, Liu Q, Bullock JM, Moon YJ, Song P, Brar SS, Madabushi R, Wu TC, Booth BP, Rahman NA, Reynolds KS, Gil Berglund E, Lesko LJ and Huang SM (2011) Applications of physiologically based pharmacokinetic (PBPK) modeling and simulation during regulatory review. Clin Pharmacol Ther 89(2): 259-67.

DMD Fast Forward. Published on March 30, 2011 as DOI: 10.1124/dmd.111.038224
This article has not been copyedited and formatted. The final version may differ from this version.

Footnotes.

Reprint requests

Hannah M Jones

Pharmacokinetics, Dynamics and Metabolism,

Pfizer Global R&D,

Ramsgate Road,

Sandwich,

Kent.

CT13 9NJ.

E-mail : Hannah.jones@pfizer.com

DMD Fast Forward. Published on March 30, 2011 as DOI: 10.1124/dmd.111.038224
This article has not been copyedited and formatted. The final version may differ from this version.

Legends for Figures.

Figure 1 : Structure of UK-369,003.

Figure 2 : Plasma PK profiles of UK-369,003 following IV infusion (A & B), IR (C & D) and MR (E & F) oral administration. Panels A, C and E show mean $^{+}/_{-}$ standard deviation. Panels B, D & F plot the corresponding data normalised to 10, 1 and 50mg respectively.

Figure 3 : Plasma PK profiles of UK-369,003 following IV infusion over 1 h. Panels A, B & C = 10, 30 & 50mg IV infusions respectively. Open symbols = observed mean data $^{+}/_{-}$ standard deviation. Solid line = model fit.

Figure 4 : Goodness of fit plots for the IV Infusion model. Panel A = weighted residual plot; Panel B = observed versus predicted plot. Solid line = unity.

Figure 5 : Plasma PK profiles of UK-369,003 following IR PO administration – ' CYP3A4 model'. Panels A-H = 1, 3, 10, 30, 100, 200, 400, 800mg respectively. Open symbols = observed mean data $^{+}/_{-}$ standard deviation. Solid line = model fit.

Figure 6 : Plasma PK profiles of UK-369,003 following IR PO administration – 'P-gp model'. Panels A-H = 1, 3, 10, 30, 100, 200, 400, 800mg respectively. Open symbols = observed mean data $^{+}/_{-}$ standard deviation. Solid line = model fit.

Figure 7 : Plasma PK profiles of UK-369,003 following IR PO administration – 'Combined model'. Panels A-H = 1, 3, 10, 30, 100, 200, 400, 800mg respectively. Open symbols = observed mean data $^{+}/_{-}$ standard deviation. Solid line = model fit.

Figure 8 : IR PO administration goodness of fit plots. Panels A & B = 'CYP3A4' model; C & D = 'P-gp' model; E & F = 'Combined' model. Panels A, C and E = weighted residual plots; Panel B, D and E = observed versus predicted plots. Solid line = unity.

Figure 9: Plasma PK profiles of UK-369,003 following MR PO administration – 'Combined' model. Panels A-C = 50, 100 & 200mg respectively. Open symbols = observed mean data $^{+}/_{-}$ standard deviation. Solid line = model fit.

Figure 10 : MR PO administration goodness of fit plots – 'CYP3A4' model. Panel A = weighted residual plot; Panel B = observed versus predicted plot. Solid line = unity.

Figure 11 : Simulated *in vivo* release from the MR device.

Figure 12 : IR PO administration – Extent of incomplete absorption, gut wall and hepatic metabolism.

Figure 13 : Panel A = Free jejunum enterocyte; Panel B = liver concentrations following administration of IR form. Horizontal line = model derived K_m.

Figure 14 : Colon luminal concentrations following administration of 100mg IR UK-369,003.

DMD Fast Forward. Published on March 30, 2011 as DOI: 10.1124/dmd.111.038224
This article has not been copyedited and formatted. The final version may differ from this version.

Tables

Table 1.

GastroPlus Input Parameters.

	UK-369,003
Effective human permeability	$2.74 * 10^4$ cm.s^{-1} [a]
Human plasma protein binding (f_{up})	66% (0.33)
Human blood:plasma ratio	1
Buffer solubility	
pH 1.1	25 mg/mL
pH 2.8	25 mg/mL
pH 4.7	25 mg/mL
pH 5.0	9.6 mg/mL
pH 6.5	0.19 mg/mL
pH 6.6	0.11 mg/mL
pH 6.7	0.1 mg/mL
pH 7.1	0.11 mg/mL
pH 7.4	0.06 mg/mL
pH 7.9	0.07 mg/mL
pH 8.8	0.11 mg/mL
pH 9.6	0.14 mg/mL
Fasted State Simulated Intestinal Fluid (FaSSIF) solubility	0.19 mg/mL

[a] estimated from Caco-2 flux in the presence of P-gp inhibitors.

DMD Fast Forward. Published on March 30, 2011 as DOI: 10.1124/dmd.111.038224
This article has not been copyedited and formatted. The final version may differ from this version.

Table 2

Pharmacokinetics of UK-369,003 following IV administration.

	Plasma Pharmacokinetics
Total Clearance	60.2 L/hr
Renal Clearance	4.2 L/hr
Vc	0.64 L/kg
Vdss	2.4 L/kg
Terminal Half-life	4 hr

DMD Fast Forward. Published on March 30, 2011 as DOI: 10.1124/dmd.111.038224
This article has not been copyedited and formatted. The final version may differ from this version.

Table 3

IV & IR oral simulation – parameter estimates and objective function measures.

	'CYP 3A4' Model	*'P-gp' Model*	*'Combined' Model*
CYP3A4 Parameter Estimates.			
Vmax (nmol/sec)	54	Not estimated	48
Km (μM)	0.64	Not estimated	0.54
P-gp Parameter Estimates.			
Vmax (nmol/sec)	Not estimated	2.0	1.0
Km (μM)	Not estimated	12.8	39
Objective Measures.			
R^2	0.89	0.38	0.89
Aikake [a]	389	688	346
Objective Function	4.65	15.2	3.93

[a] Aikake = $N_{observations}$ * ln(Objective function) + 2*($N_{parameters}$)

Figure 1.

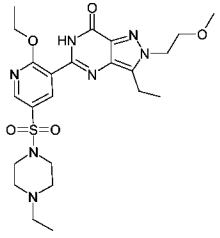

Figure 2.

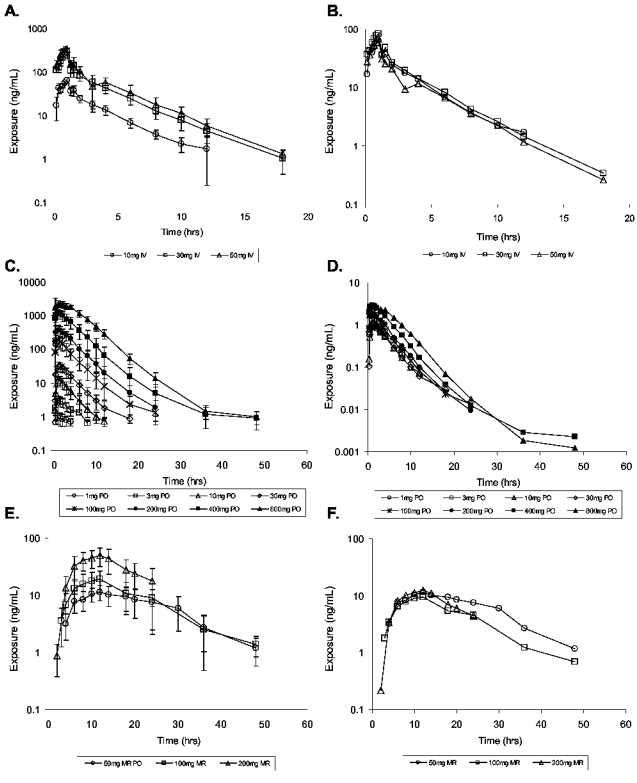
A.
Exposure (ng/mL)
Time (hrs)
10mg IV
30mg IV
60mg IV
B.
Exposure (ng/mL)
Time (hrs)
10mg IV
30mg IV
60mg IV
C.
Exposure (ng/mL)
Time (hrs)
1mg PO
3mg PO
10mg PO
30mg PO
100mg PO
200mg PO
400mg PO
800mg PO
D.
Exposure (ng/mL)
Time (hrs)
1mg PO
3mg PO
10mg PO
30mg PO
100mg PO
200mg PO
400mg PO
800mg PO
E.
Exposure (ng/mL)
Time (hrs)
50mg MR PO
100mg MR
200mg MR
F.
Exposure (ng/mL)
Time (hrs)
50mg MR
100mg MR
200mg MR

Figure 3.

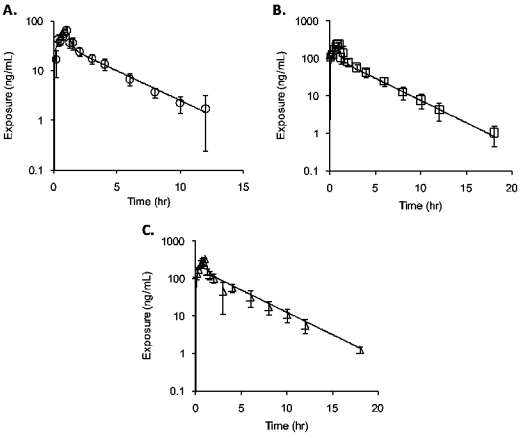
A.
Exposure (ng/mL)
100
10
1
0.1
0
5
10
15
Time (hr)
B.
Exposure (ng/mL)
1000
100
10
1
0.1
0
5
10
15
20
Time (hr)
C.
Exposure (ng/mL)
1000
100
10
1
0.1
0
5
10
15
20
Time (hr)

Figure 4.

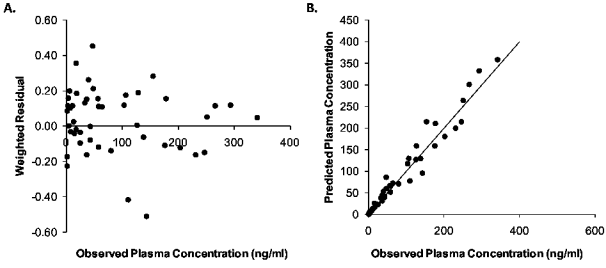
A.
Weighted Residual
0.60
0.40
0.20
0.00
-0.20
-0.40
-0.60
0
100
200
300
400
Observed Plasma Concentration (ng/ml)
B.
Predicted Plasma Concentration
450
400
350
300
250
200
150
100
50
0
0
200
400
600
Observed Plasma Concentration (ng/ml)

Figure 5.

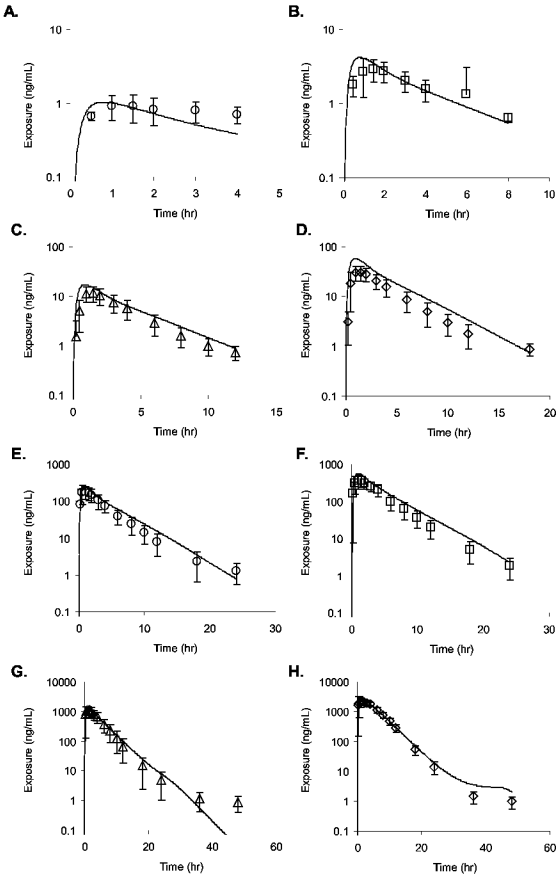

Figure 6.

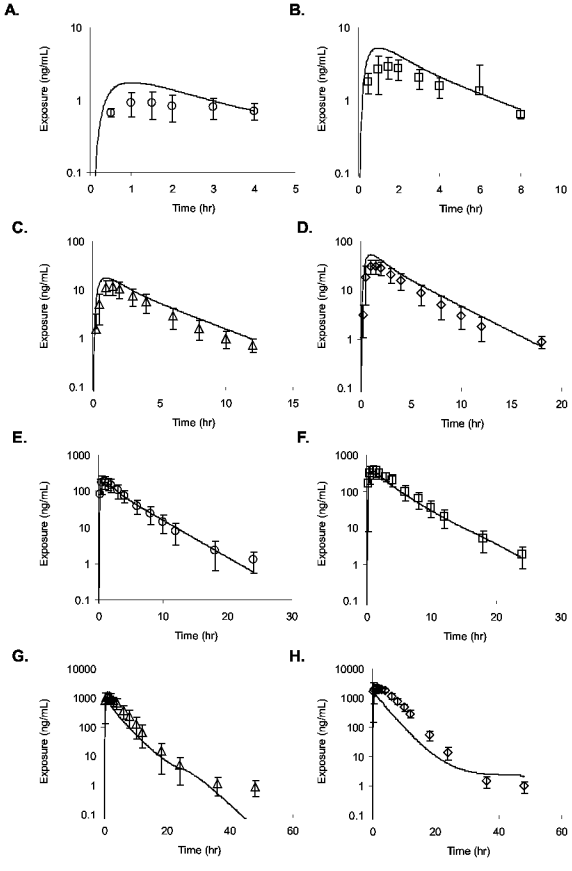

Figure 7.

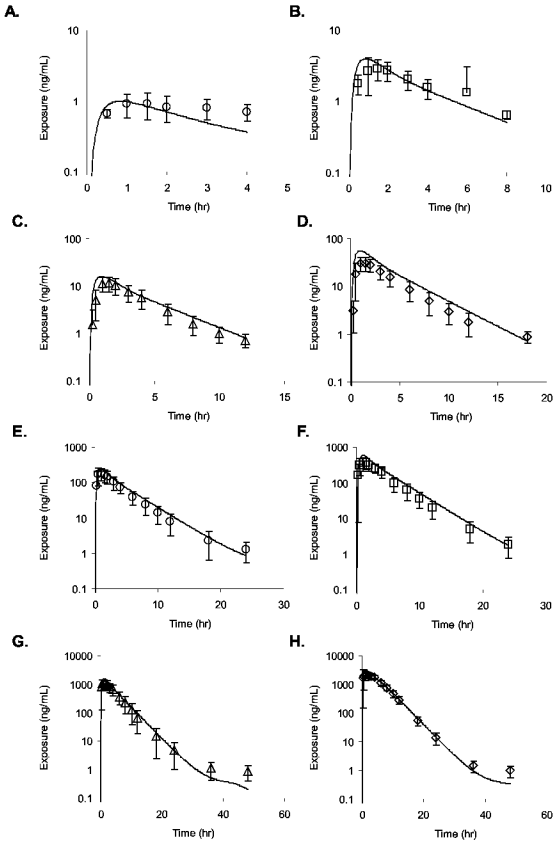

Figure 8.

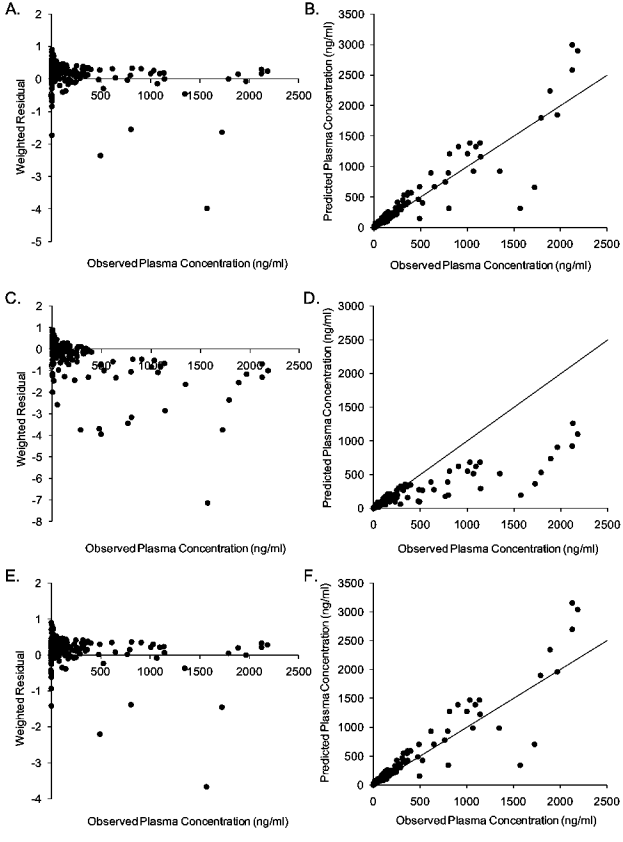
A.
Weighted Residual
Observed Plasma Concentration (ng/ml)
B.
Predicted Plasma Concentration (ng/ml)
Observed Plasma Concentration (ng/ml)
C.
Weighted Residual
Observed Plasma Concentration (ng/ml)
D.
Predicted Plasma Concentration (ng/ml)
Observed Plasma Concentration (ng/ml)
E.
Weighted Residual
Observed Plasma Concentration (ng/ml)
F.
Predicted Plasma Concentration (ng/ml)
Observed Plasma Concentration (ng/ml)

Figure 9.

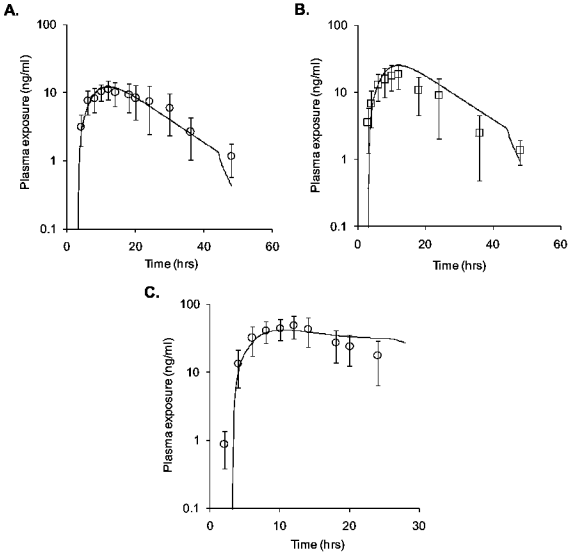
A.
Plasma exposure (ng/ml)
100
10
1
0.1
0
20
40
60
Time (hrs)
B.
Plasma exposure (ng/ml)
100
10
1
0.1
0
20
40
60
Time (hrs)
C.
Plasma exposure (ng/ml)
100
10
1
0.1
0
10
20
30
Time (hrs)

Figure 10.

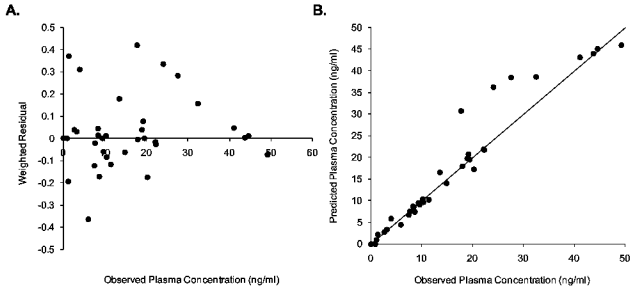
A.
Weighted Residual
0.5
0.4
0.3
0.2
0.1
0
-0.1
-0.2
-0.3
-0.4
-0.5
0
10
20
30
40
50
60
Observed Plasma Concentration (ng/ml)
B.
Predicted Plasma Concentration (ng/ml)
50
45
40
35
30
25
20
15
10
5
0
0
10
20
30
40
50
Observed Plasma Concentration (ng/ml)

Figure 11.

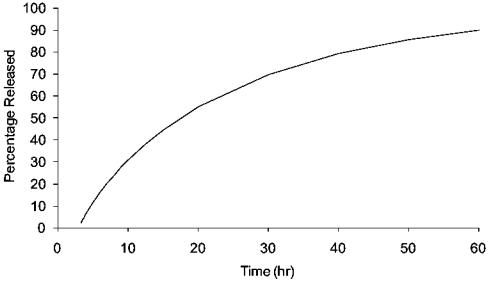
Percentage Released
100
90
80
70
60
50
40
30
20
10
0
0
10
20
30
40
50
60
Time (hr)

Figure 12.

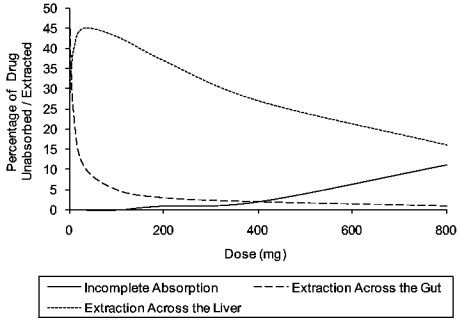
Percentage of Drug Unabsorbed / Extracted
50
45
40
35
30
25
20
15
10
5
0
0
200
400
600
800
Dose (mg)
Incomplete Absorption
Extraction Across the Gut
Extraction Across the Liver

Figure 13.

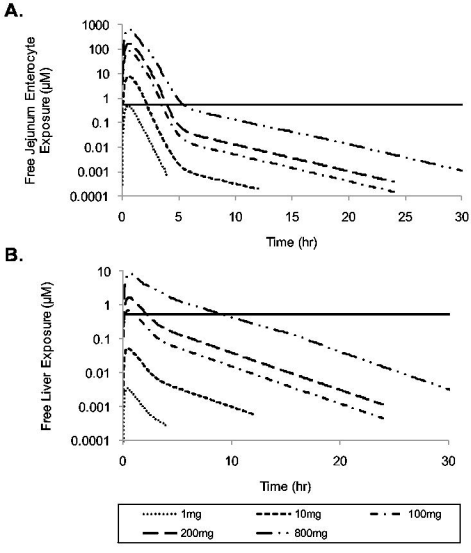
A.
Free Jejunum Enterocyte Exposure (µM)
1000
100
10
1
0.1
0.01
0.001
0.0001
0
5
10
15
20
25
30
Time (hr)
B.
Free Liver Exposure (µM)
10
1
0.1
0.01
0.001
0.0001
0
10
20
30
Time (hr)
1mg
10mg
100mg
200mg
800mg

Figure 14.

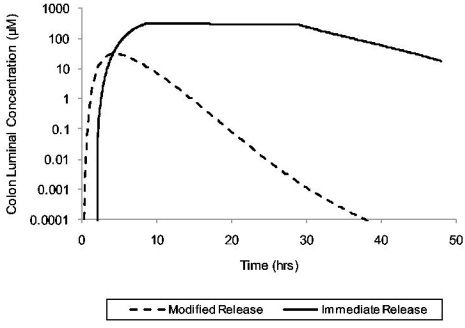
Colon Luminal Concentration (μM)
1000
100
10
1
0.1
0.01
0.001
0.0001
0
10
20
30
40
50
Time (hrs)
Modified Release
Immediate Release